JAERI-M

8944

DESIGN PROBLEM OF HIGH HEAT FLUX DIVERTOR STRUCTURE

July 1980

Hiromasa IIDA, Akio MINATO*
Hiroki SAKAMOTO** and Kiyoshi SAKO

日本原子力研究所
Japan Atomic Energy Research Institute

Design Problem of High Heat Flux Divertor Structure

Hiromasa IIDA, Akio MINATO*, Hiroki SAKAMOTO** and Kiyoshi SAKO

Division of Thermonuclear Fusion Research, Tokai Research Establishment, JAERI

(Received June 13,1980)

Poloidal divertor is a promising method for impurity control and ash-exhaust in a Tokamak fusion reactor. However engineering design of divertor neutralizer plate has severe problems due to very high heat flux, erosion and damage of material by ion sputtering and neutron irradiation and strong electromagnetic forces with plasma disruptions. In this report we discuss engineering problems on the bases of INTOR-J design and propose some method to solve the problems.

Keywords: Tokamak Fusion Reactor, INTOR, Poloidal Divertor, Electromagnetic Force, Erosion ,Ion Sputtering, Neutralizer Plate.

* On leave frome Kawasaki Heavy Industries,Ltd.

** On leave from Mitsubishi Heavy Industries,Ltd.

高熱流束ダイバータの工学的問題点の検討

日本原子力研究所東海研究所核融合研究部
飯田浩正・湊　章男*
坂本寛己**・迫　　淳

（1980年6月13日受理）

ポロイダルダイバータは，トカマク炉の不純物制御，灰除去のための有力な方法とされている。しかし，ポロイダルダイバータは，高熱流束を受ける，強い電磁力を受ける，およびイオンスパッタリングによる浸食が大きい，中性子による放射線損傷を受けるなどの工学的問題がある。INTOR－J のダイバータ設計を基にそれらを検討し，対策の試案について述べた。

＊　外来研究員：川崎重工業（株）
＊＊　〃　：三菱重工業（株）

CONTENTS

1. Introduction

Poloidal divertor is said to be a promising method for impurity control and ash-exhaust in a Tokamak fusion reactor[1]. However engineering design of divertor neutralizer plate has severe problems due to very high heat flux, erosion and damage of material by ion sputtering and neutron irradiation and strong electromagnetic forces with plasma disruptions. In this report we discuss engineering feasibility of poloidal divertor.

Figure 1 shows a bird's-eye view of INTOR-J[2], Japanese proposal for International Tokamak Reactor (INTOR). Hitach Ltd. conducted a design study of divertor neutralizer under contract with JAERI. Design conditions assumed are as follows.

Heat load 50 MW (total) carried by ions and electrons
- duration : 200 S
- dwell time : 100 S
- Pulse shape : step function
- spatial distribution : Gaussian with 10 cm of FWHM
- incident angle of particles to the horizontal plane : 5°
- swinging frequency and span : 1 Hz and 10 cm
- Plasma disruption time constant : 10 msec
- Particle flux on the divertor plate : $1.5 \times 10^{21}/m^2 \cdot s$
- Mean energy of ions impacting divertor plate : 1.3 keV

Cross sectional view and bird's-eye view of the divertor plate are shown in Fig.2 and Fig.3. Thirty -two neutralizer plates are installed in each reactor module which forms 1/6 part of a reactor. The plate in outboard of torus consists of 28 cooling tubes and the inboard plate 24 cooling tubes. The plates are installed not normally to the projected ion beam line to the vertical plane in order to lessen the heat flux on them. The angle between the projected beam line and the normal of the plate is 70 degree. The size of these plates are determined by taking into account the width of scrape-off layer at divertor plate, the space available for the plate between plasma and toroidal field coil and remote handling operation required for their replacement. The cross section of a cooling tube and steady-state temperature distribution are shown in Fig.4[3]. As shown in this figure, one side of cooling tube is tapered with an angle of 7.5° to prevent the melting of a tube edge when it bends slightly by some causes and protrudes out of the plate surface. The heat fluxes on the flat and tapered parts are 160 w/cm^2 and 400 w/cm^2, respectively. Because of these very high heat fluxes the material of the tube has to have good heat conductance. Copper is selected for this reason. The maximum temperature in the divertor plate is about 250 °C. The temperature difference between the surface (A) and the coolant channel wall (D) in Fig.4 is 60 °C. The thermal stress caused by this temperature difference is a little below the proven stress of copper 7 kg/mm^2. The maximum heat flux at channel wall is about 450 w/cm^2. Figure 5 shows the burn out heat flux of pressurized water cooling.

The above design has following problems.

(1) The buckling of cooling tube has to be severely limited so that the δ in Fig.6 is kept smaller than 0.6 mm.

(2) The interaction between the toroidal fields and the eddy current induced in the divertor plate produces vertical forces as shown in Fig.7. The induction voltage in the divertor plate due to disruption of a 4.7-MA plasma with 10-msec time constant is expected to be 1.4 volt taking into account the effect of the eddy current in the vacuum vessel which retard the change of magnetic flux at divertor plate. Rough estimation shows that the vertical force at the edge of the plate will be 6.4 t/m with copper headers and 1.4 t/m with stainless steel headers.[4] These forces must be reduced significantly in some way.

(3) Erosion of the neutralizer plate in a year is estimated as Follows[5]

$$d=\frac{\phi}{s}\cdot T\cdot Av\cdot\frac{1}{N_o}\cdot\frac{M}{\rho}\cdot S_y\cdot P \qquad \text{-----------} (1)$$

where

d ; depth of erosion (cm)

ϕ ; integrated particle flux to divertor ($1\times10^{23}s^{-1}$)

s ; surface area of neutralizer plate ($70.7m^2$;INTOR-J)

T ; 3.15×10^7sec

Av; availability (0.25)

N_o; Avogadro's Number (6.023×10^{23})

M ; atomic weight (63.5)

ρ ; density (8.93g/cc)

Sy; sputtering yield (0.1 for D^+ and~0.15 for T^+ at 1.3KeV)

P ; peaking factor of ion's spatial distribution on the plate (1.0 : ion beam line will be swung with 1 Hz)

This leads to 17mm/year of erosion of the divertor plate. Sputtering yield data of copper for T^+ is not available and assumed to be one and a half as large as that for D^+. The life time of divertor plate will be very short.

(4) Figure 8 shows temperature rise at the center of the divertor plate after reactor start up. Figure 9 shows a distribution of thermal stress in the plate at 0.02 sec after reactor start up. Repetitive thermal stress due to pulsive operation of the reactor might lower the life time of the divertor plate to 3~4 months.

(5) Radiation damage of the plate due to 14 MeV neutron irradiation, especially swelling of copper, could be a serious problem. Though it is now difficult to make accurate evaluation of its effect on the life time because of lack of the radiation damage data for copper.

(6) In Hitachi Ltd's design remote maintenance procedure of divertor plate is studied in detail[(2)]. In the procedure cutting and welding of the irradiated material is required. The welding of irradiated material with a significant deal of helium could be very difficult.

(7) Neutralizer plates need to be installed to a reactor with very high accuracy not to produce unnecessary peaking of heat flux. Once reactor is operated with D-T burning this must be done with full remote handling.

2. Design study of divertor plate with suggested parameters for INTOR by the physics group

The physics group suggested two sets of divertor heat load parameter at the previous March session. We employ here those of case A which is more severe conditions for divertor plate design than case B. The following are case A parameters.

	A
Radiation	15 MW
Charge Exchange	5-10 MW
Power to divertor (charged particles)	100 MW
Mean charge-exchange neutral energy	300 eV
Scrape-off temperature	300 eV
Particle flux to divertor (ions)	$2 \times 10^{23} s^{-1}$
Mean energy of ions impacting divertor plate	1.3 keV

We assume following in addition to the above.

saptial distribution of ions impacting the plate
: Gaussian with 10 cm of FWHM.

plasma disruption time constant : 20 msec.

2.1 Some improvements for solving design problems

2.1.1 Prevention of cooling tube buckling

Since the heat load in the case A is twice as large as that assumed for INTOR-J, heat fluxes on the flat and tapered part will be ~310 w/cm^2 and ~770 w/cm^2, respectively with slight modification concerning with the diference of major radius, i.e. area of divertor plate. If we attach some tubes at the back of the plate transversly to the copper cooling tubes as shown in Fig.10 and prevent the buckling of copper tubes, tapering of the tube may not be necessary. Then the maximum heat flux on the divertor plate will be 310 w/cm^2.

2.1.2 Cooling tube shape for heat flux flattening

The spatial distribution of the heat load on the plate is assumed to be Gaussian as shown in Fig.11. If the peak of heat load is always on the center of the plate, S-shaped cooling tube as shown in Fig.12 provides flat heat load distribution. The maximum heat flux with using S-shaped tube will be a half of that in case of straight tube. However, when the peak of the distribution moves and is off the center of the plate the maximum heat flux become rather high as shown in Fig.13. We assumed here that 4 cm of particle beam deviation can be possible and selected the cooling tube shape as shown in Fig.14. That shape gives us 280 w/cm^2 of maximum heat flux on the divertor plate.

2.1.3 Reduction of electromagnetic force on the plate

One of the methods which can reduce the electromagnetic force induced on the plate is to increase the electric resistance of cooling tubes. Table 1 shows electrical and thermal characteristics of copper and stainless-steel. The use of thin stainless steel tube at the part where heat flux is not expected to be very high increases the electrical resistance.

2.1.4 Protection of the plate against erosion by ion sputtering

Erosion of the copper divertor plate will be 56mm/year at the center assuming parameters in the case A, 25% of availability and 1.7 of peaking factor of ion's spatial distribution on the plate.

Some metal such as Molybdenum which has small sputtering yield, attached on the divertor plate as shown in Fig. 15 could increase life time of the plate. Erosion of TZM attached on the plate will be ∿ 4.5mm/year. This gives not sufficiently long life time of the plate yet. Even in the optimistic case suggested by physics group with 450 eV of ion energy impacting erosion of TZM will only become half of 4.5mm/year and be severe problem.

2.2 Preliminary design of divertor plate

2.2.1 Structure of the plate

Figure 16 shows the cross section of divertor plate room. Structure of inboard and outboard divertor plates are shown in Fig. 17 and Fig. 18, respectively. The plate consists of two stainless steel headers, rather flexible cooling tubes made of copper and stainless steel and support tubes made of stainless steel.

2.2.2 Thermal analysis

Heat flux at the center of the plate will be ∿ 280W/cm^2 as estimated previously. The temperature distribution in case of INTOR-J as shown in Fig 4 has been calculated by assuming 160W/cm^2 on flat part ,400W/cm^2 on tapered part and 280W/cm^2 on average. We estimate the temperature distribution here from Fig. 4. Figure 19 is an estimated temperature distribution. The temperature difference between the surface (A) and the coolant channel wall (D) in Fig. 19 is ∿ 40°C which does not cause problem for the thermal stress. The maximum heat flux at the coolant channel will be less than that of INTOR-J.

2.2.3 Stress analysis

An internal pressure of coolant(5 ata), thermal load and electromagnetic force act on the divertor structure. Taking account of the above loads and force, the stress analysis has been carried out.

(1) Analytical model

Figure 20 shows the two dimensional analytical model of outer divertor structure shown in Fig. 8. The cross sections and materials of each tube are shown in Table 2 . In this stress analysis, the pipe element in SAP-V is employed.

(2) Analytical conditions

(a) Thermal load

The temperature difference occurs between front and back side in the copper tube(divertor tube in Fig.8) by surface heat flux. The temperatures at the front and back side are about 240°C and 160°C, respectively. But, we assumed in this analysis that the temperature of the copper tube is uniform in the circumferencial direction and the temperature of the header and connection tube is 80°C (inlet temperature).

Moreover, the temperature distribution produced in the copper tube is not uniform in the longitudinal direction. It depends on the shape of distribution of the surface heat flux. The maximum temperature occurs at the center point and the minimum temperature at each end.

(b) Electro magnetic force

In order to estimate the electro magnetic force, the resistances of each tube shown in Fig.8 were calculated, assuming that an electrical insulation is provided between the support tube and divertor tube. The resistances of the divertor tube, connection tube and header are shown in Table 3. The total resistance between main support tubes shown in Fig. 21 is 1.49×10^{-2} Ω. The electromotive force generated in the divertor structure is 0.716 V at the plasma disruption.
The eddy current is 48 A (= $0.716/1.49^{-2}$). Therefore, the electro-magnetic force generated is 240 N/m (toroidal field : $5 Wb/m^2$).

(c) Internal pressure load

The internal pressure of the coolant(pressurized water) is 5 kgf/cm^2. Since it is small, it is neglected in this analysis.

The material properties of 316 ss and copper used in this stress analysis are shown in Table 1.

(3) Analytical results

Figures 22 and 23 show the pre and post deformation shape under the electro magnetic force and thermal load (maximum temperature : 160°C). The stresses at the typical positions are shown in Table 4.

Since the electro magnetic force is small, the stress induced is lower than an allowable stress. But, if the temperature difference in the copper tube(divertor tube) is taken into account, the thermal stress induced in each tube will increase. More detailed stress analysis and optimum structure selection such as connection tube (node 2) to reduce the thermal stress will be neccessary.

2.2.4 Installation of divertor plates

The plate will be installed with some gap between adjacent plates. To prevent the additional high heat fulx on the edge of the plate, level difference will be required as shown in Fig. 24. Figure 24 shows relationship of gap and required level difference for it. The gap width is assumed here to be 12mm and level difference must be more than 1.05mm. It should be noted that if we make level difference be 5mm allowing some margin the average heat flux on the plate increase 10%. High accuracy is required for installation of the divertor plate.

3. Conclusion

(1) It is possible to prevent the protrusion of the divertor cooling tube by reinforcing with the support tube attached transversely to the cooling tube at the back of the plate (tube assembly).

(2) The partial use of thin stainless steel tube in a cooling tube reduces sufficiently electromagnetic force induced on the plate. But some effort must be paid to obtain sufficient electrical resistance at the interface between the cooling and support tubes.

(3) By selecting appropriate shape of tubes the heat flux on the plate can be decreased and large heat flux peaking can be prevented even when some fluctuation of beam line occurred.

(4) When the copper cooling tube receives the heat flux of 280 w/cm^2 which is estimated using the case A parameters and taking into account of the space available for the plate,the tube can be cooled by water of 5 ata and the thermal stress caused on the plate can be smaller than allowable stress.

(5) TZM or Nb alloy attached on the surface of the plate can increase life time of the plate. However, it is important to develop the method to lower the particle energy impacting on the surface of the plate to reduce erosion due to sputtering.

(6) Though the radiation damage of copper can not be evaluated accurately so far but it could be severe problem. If heat flux on the plate become lower significantly (the case B) we can use thin stainless steel tube (0.6 mm) inside the copper tube and the problem of radiation damage of copper will not be severe.

(7) Positioning of the plate in a reactor requires high accuracy and remote handling technique must be fully developed.

(8) Welding of irradiated stainless steel header may be possible but should be investigated sufficiently.

(9) The span of the particle beam fluctuation affect the plate design severely. It should be predicted accurately how large the fluctuation will be.

(10) Spatial distribution of the particle flux also affect the plate design. It should be also investigated.

(11) If the width of scrape-off layer become 5 cm, the allowable beam fluctuation span will be half and more accuracy will be required for positioning of the plate in a reactor.

(12) Thermal stress should be sufficiently small taking into account of the fatigue of material.

REFERENCE

(1) Y. SHIMOMURA, K. SAKO and K. SHINYA, JAERI-M 8294 (1979)

(2) K. SAKO, T. TONE, Y. SEKI, H. IIDA, et.al., JAERI-M 8518 (1979)

(3) M. KOIZUMI et. al., Annual Meeting, Japan Atomic Energy Soc., D33 Mar. 1980.

(4) T. KOBAYASHI , private communication.

(5) K. MAKI, private communication.

Table 1 Material properties of 316 ss and copper

Material	Young's modulus (kgf/mm^2)	Poison's ratio	Mean thermal expansion coefficient (/°C)	Resistivity (Ω.m)
316 ss	18000	0.3	1.95×10^{-5}	72×10^{-8}
copper	11000	0.33	1.67×10^{-5}	1.67×10^{-8}

Table 2 Cross sections and materials of each tube

Group@	Element node No.	Out dia. (mm)	Thickness (mm)	Material
1	2 - 3	12.0	1.0	316 ss
2	3 - 5	20.0	5.0	copper
2	5 - 6	20.0	5.0	copper
2	6 - 9	20.0	5.0	copper
2	9 - 10	20.0	5.0	copper
2	10 - 12	20.0	5.0	copper
2	12 - 14	20.0	5.0	copper
2	14 - 16	20.0	5.0	copper
2	16 - 18	20.0	5.0	copper
1	18 - 19	12.0	1.0	316 ss
1	19 - 21	12.0	1.0	316 ss
1	21 - 24	12.0	1.0	316 ss
1	22 - 23	12.0	1.0	316 ss
1	23 - 24	12.0	1.0	316 ss
3	20 - 22	30.0	5.0	316 ss
3	2 - 4	30.0	5.0	316 ss
3	4 - 7	30.0	5.0	316 ss
3	7 - 8	30.0	5.0	316 ss
3	8 - 11	30.0	5.0	316 ss
3	11 - 13	30.0	5.0	316 ss
3	13 - 15	30.0	5.0	316 ss
3	15 - 26	30.0	5.0	316 ss
3	17 - 26	30.0	5.0	316 ss
3	17 - 20	30.0	5.0	316 ss
4	17 - 18	20.0	5.0	316 ss
4	14 - 15	20.0	5.0	316 ss
4	12 - 13	20.0	5.0	316 ss
4	10 - 11	20.0	5.0	316 ss
4	5 - 7	20.0	5.0	316 ss

@ Group 1 : Connection tube, Group 2 : Divertor tube, Group 3 : Main support tube, Group 4 : Connection support tube

Table 3 Resistance of each tube

Name	Material	Length (m)	Section area(m^2)	Resistivity ($\Omega\cdot m$)	Resistance (Ω)
Connection tube	316 ss	0.35	3.46×10^{-5}	72×10^{-8}	7.29×10^{-3}
Divertor tube	copper	0.55	2.79×10^{-4}	1.72×10^{-8}	3.40×10^{-5}
Header	316 ss	0.62	3.46×10^{-3}	72×10^{-8}	1.29×10^{-4}

Table 4 Stresses at the typical positions

Position (node No.)	Material	Electro magnetic force	Thermal load 160°C	Thermal load 200°C
2	316 ss	-0.034	-18.000	-27.000
5	copper	-0.394	-5.669	-8.504
15	316 ss	0.540	-10.581	-15.872
21	316 ss	0.698	4.262	6.393
22	316 ss	-1.256	-5.319	-7.979

Unit : kgf/mm^2

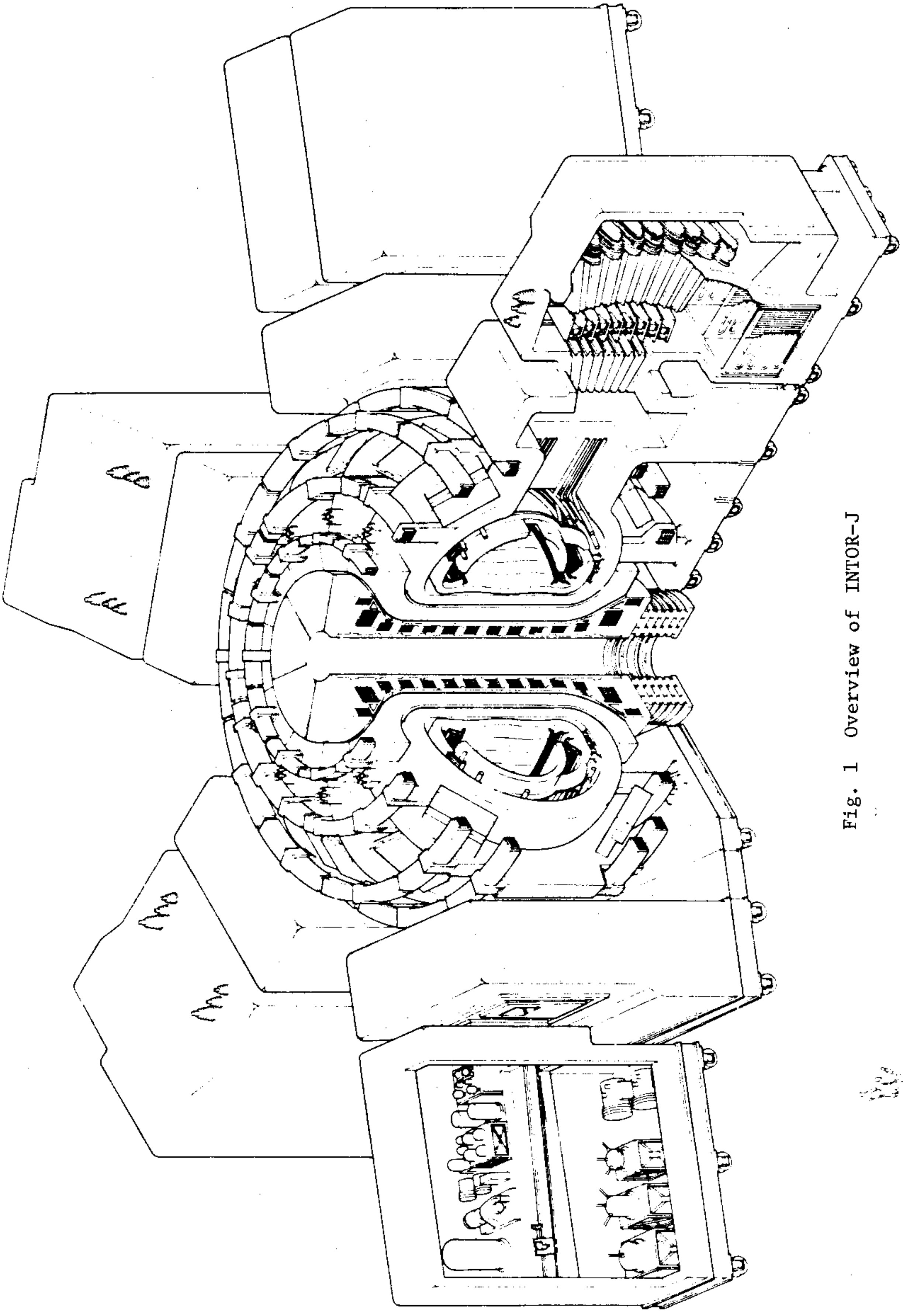

Fig. 1 Overview of INTOR-J

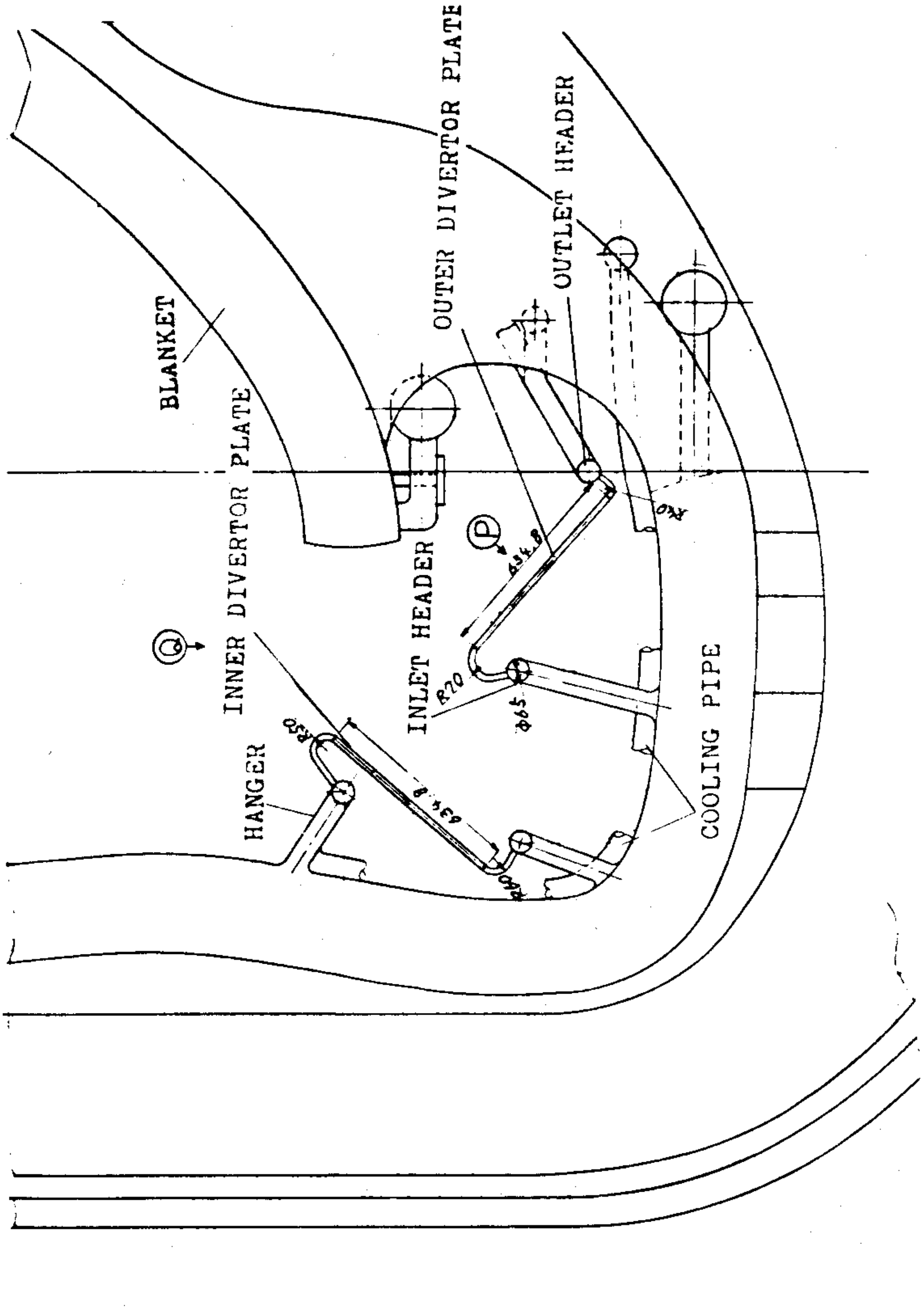

Fig. 2. Arrangement of Divertor Plate

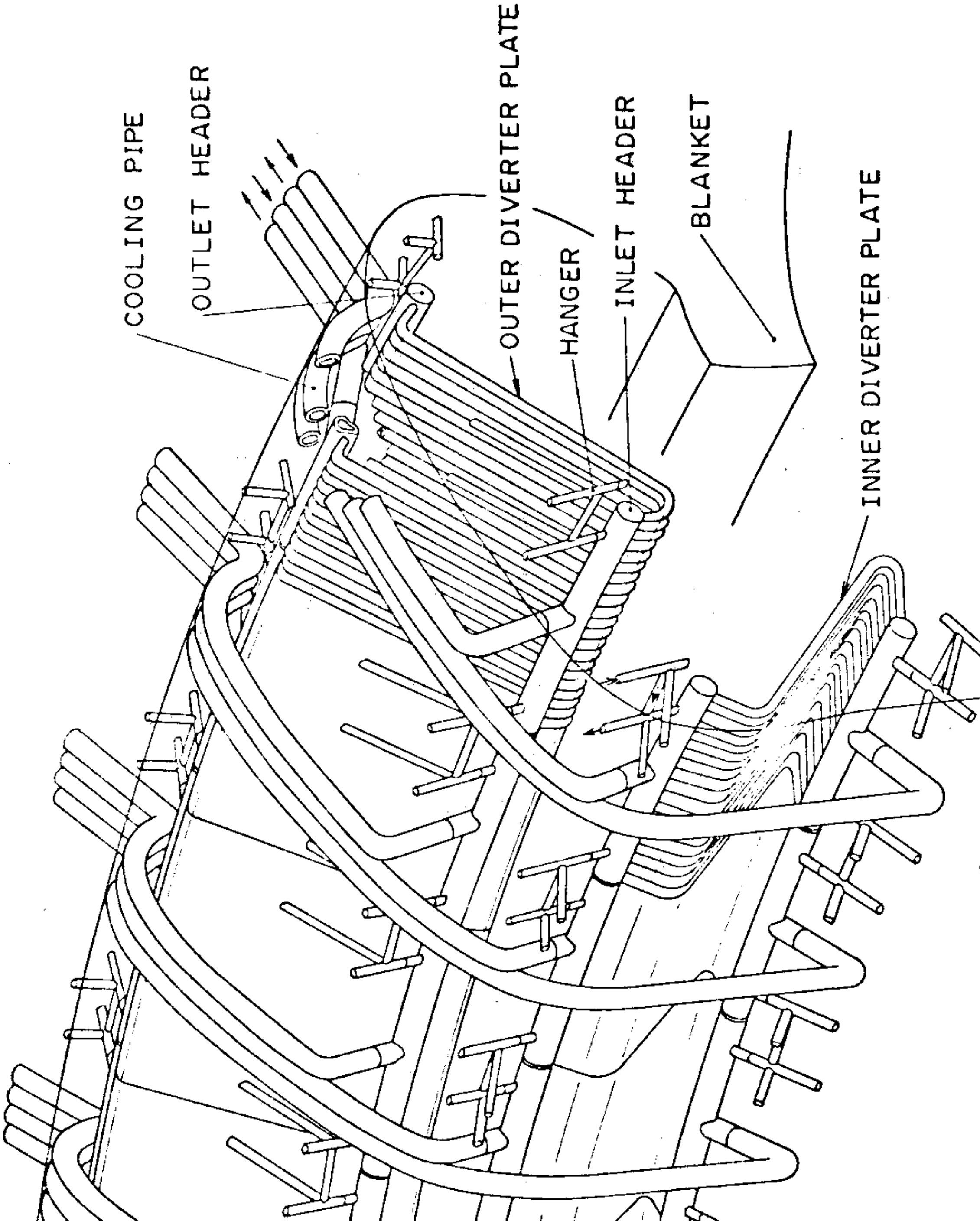

Fig. 3 Divertor plate

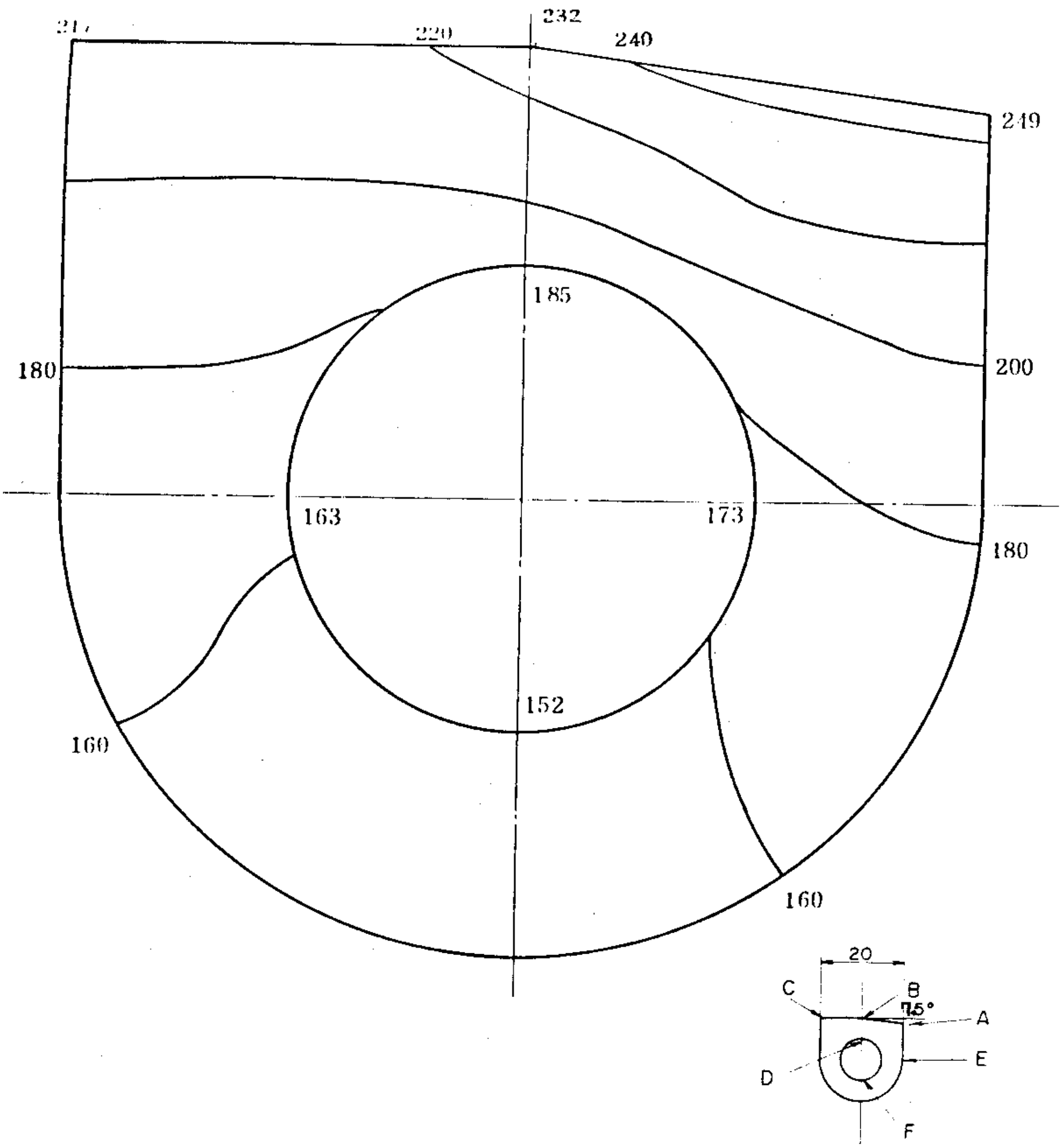

Fig. 4 Temperature distribution in the cooling tube

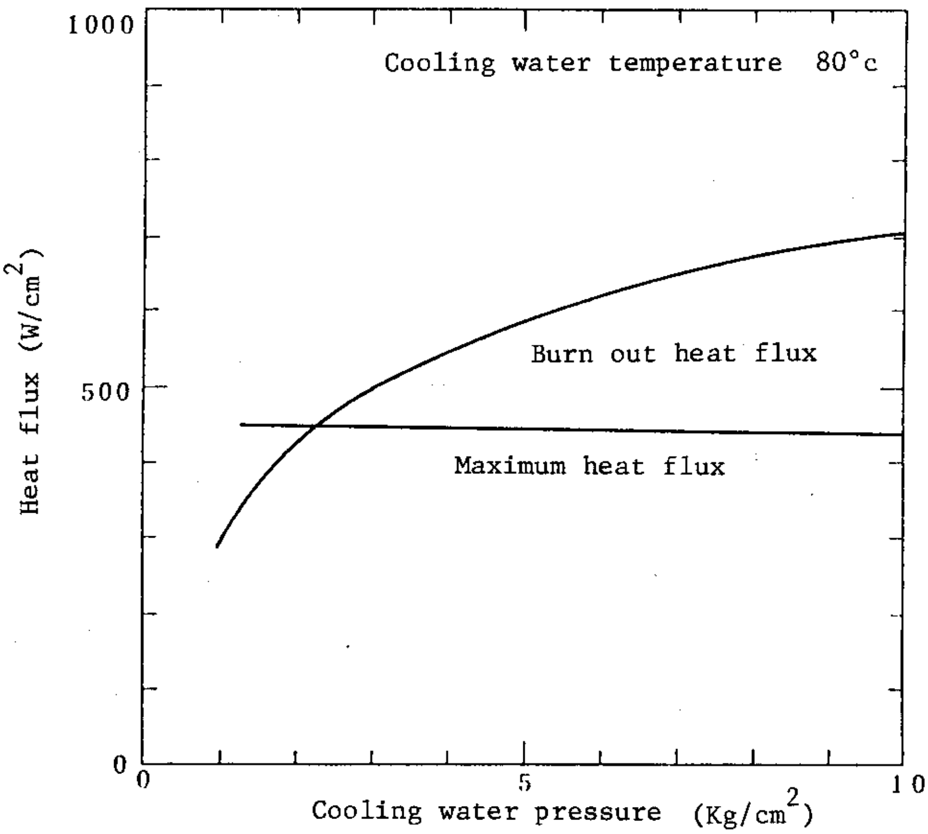

Fig. 5 Burn out heat flux of pressurized water

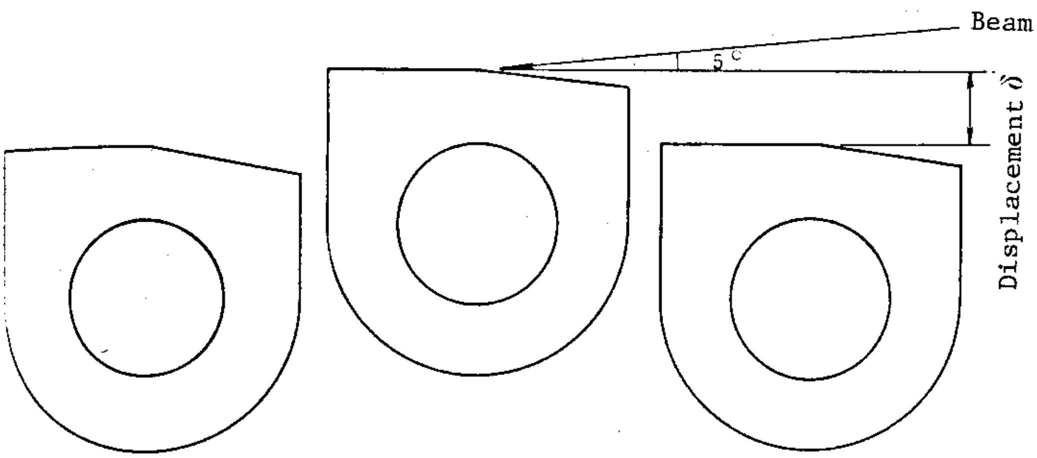

Fig. 6 Protrusion of one of the cooling tube

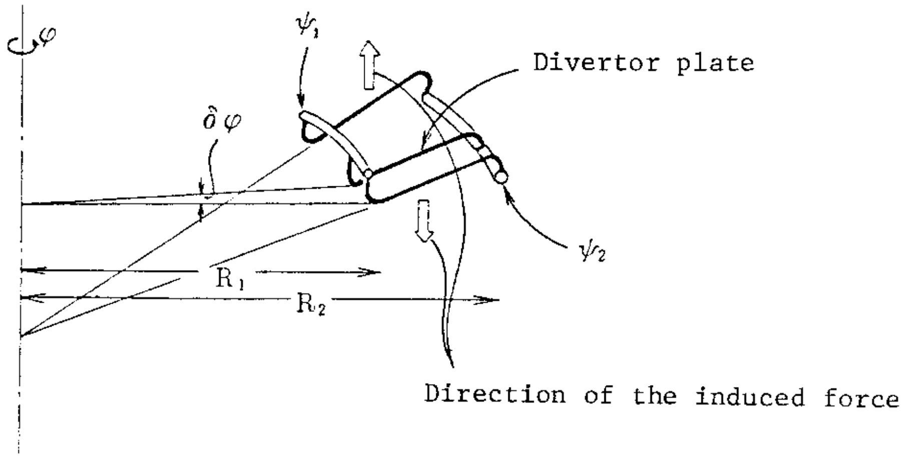

Fig. 7 Electromagnetic force induced on the divertor plate

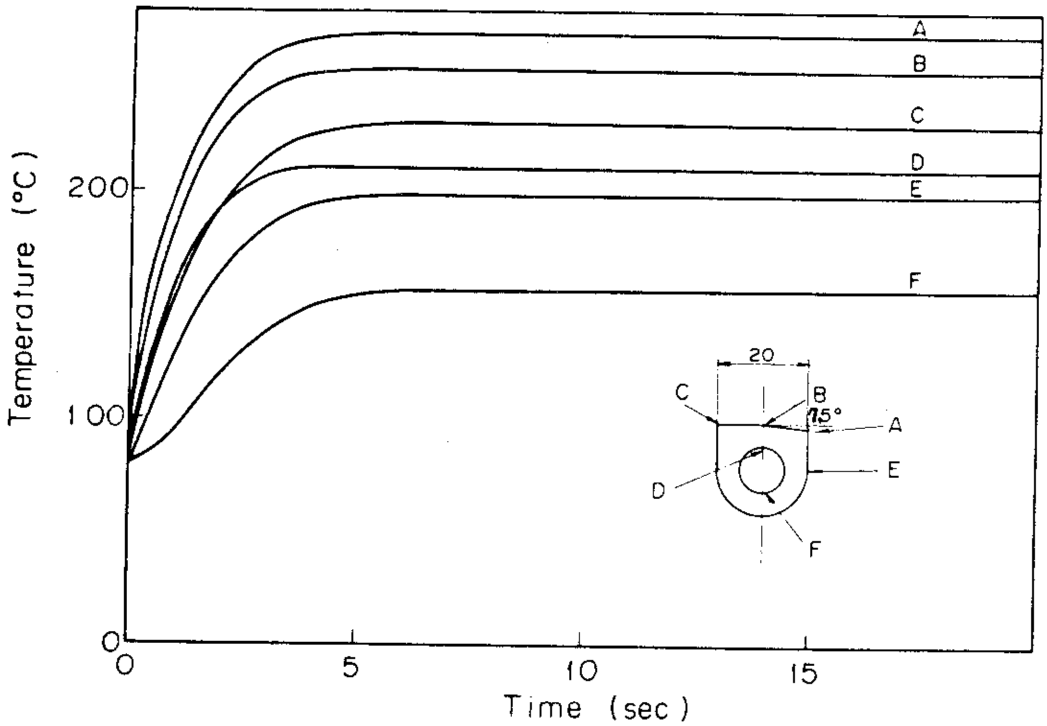

Fig. 8 Temperature Rise at the Center of the Divertor Plate Where the Largest Heat Flux Comes

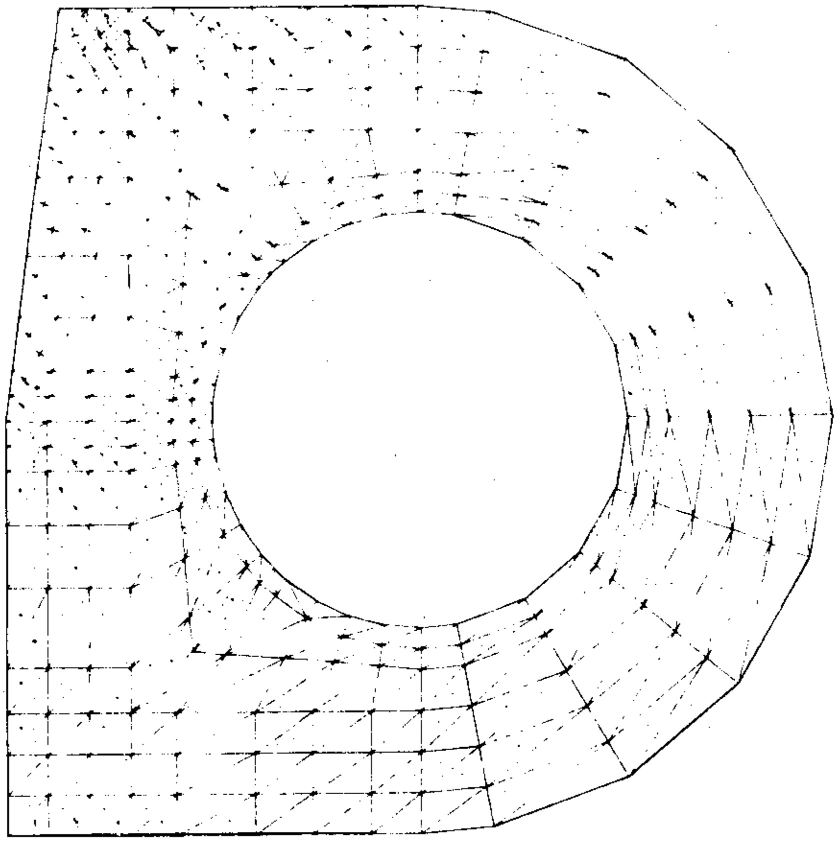

Fig. 9 Distribution of Thermal Stress in the Divertor Plate at 0.02S after Start of Irradiation

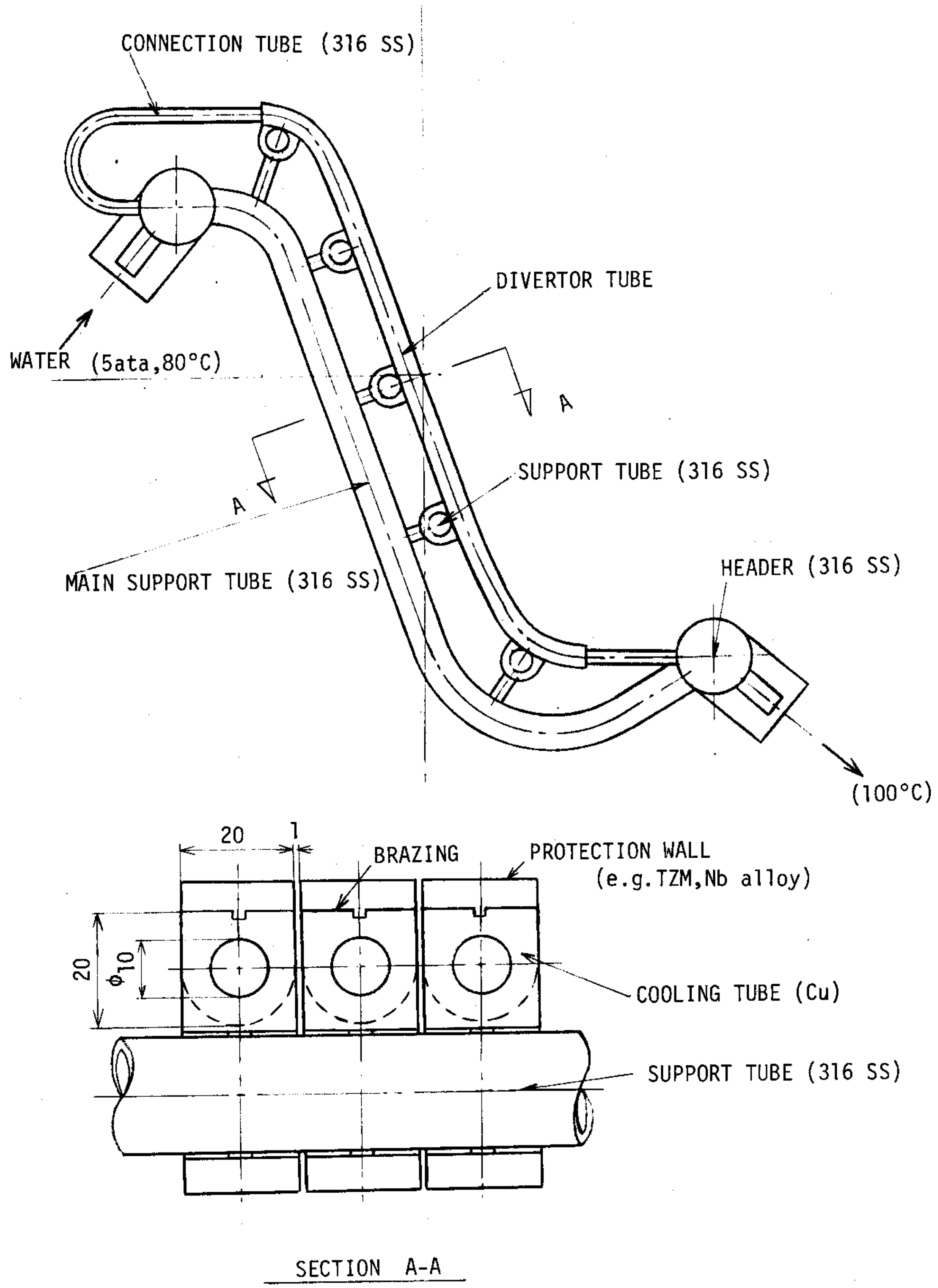

Fig. 10 Prevention of cooling tube buckling

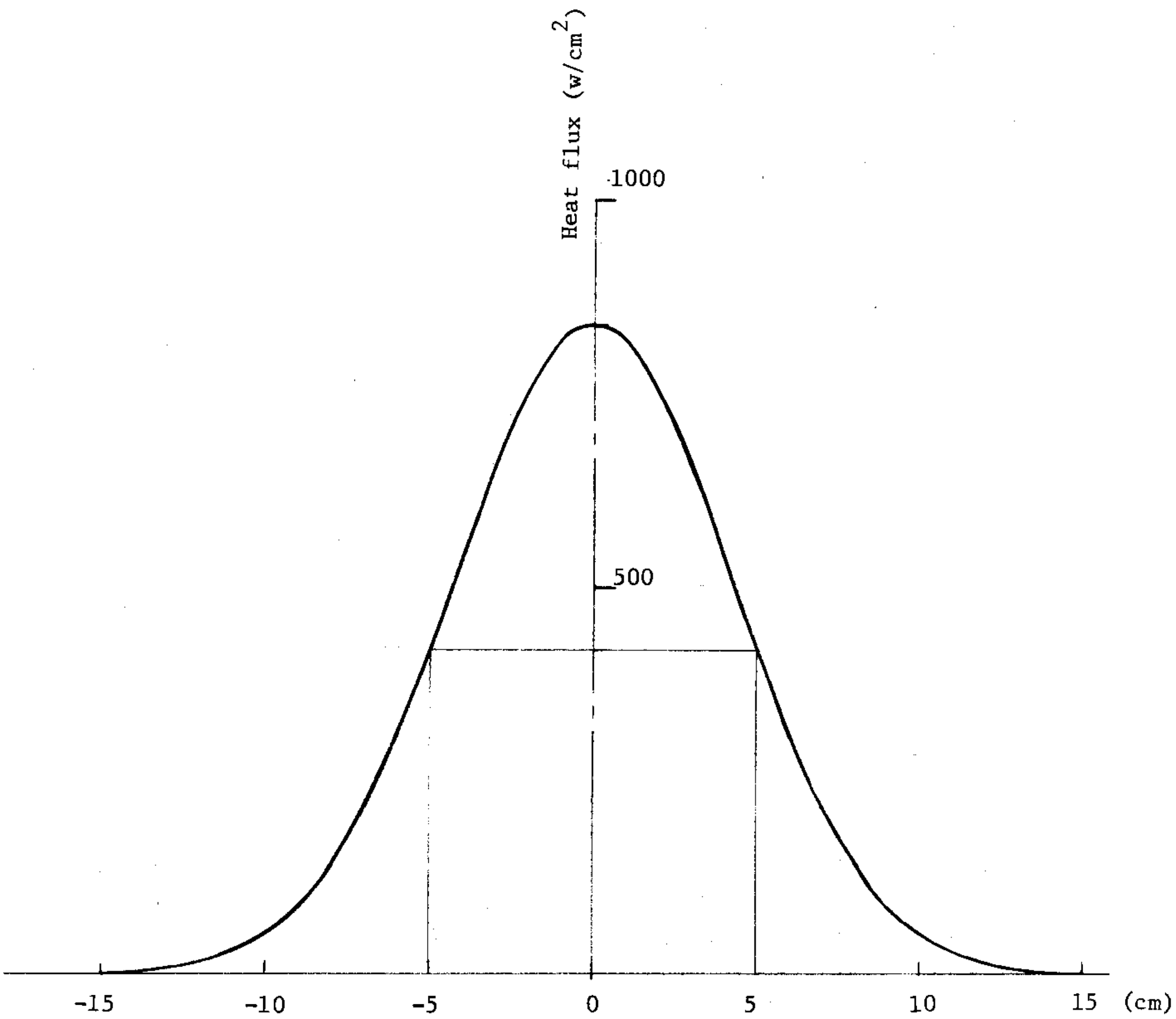

Fig. 11 Assumed heat flux distribution (Gaussian)

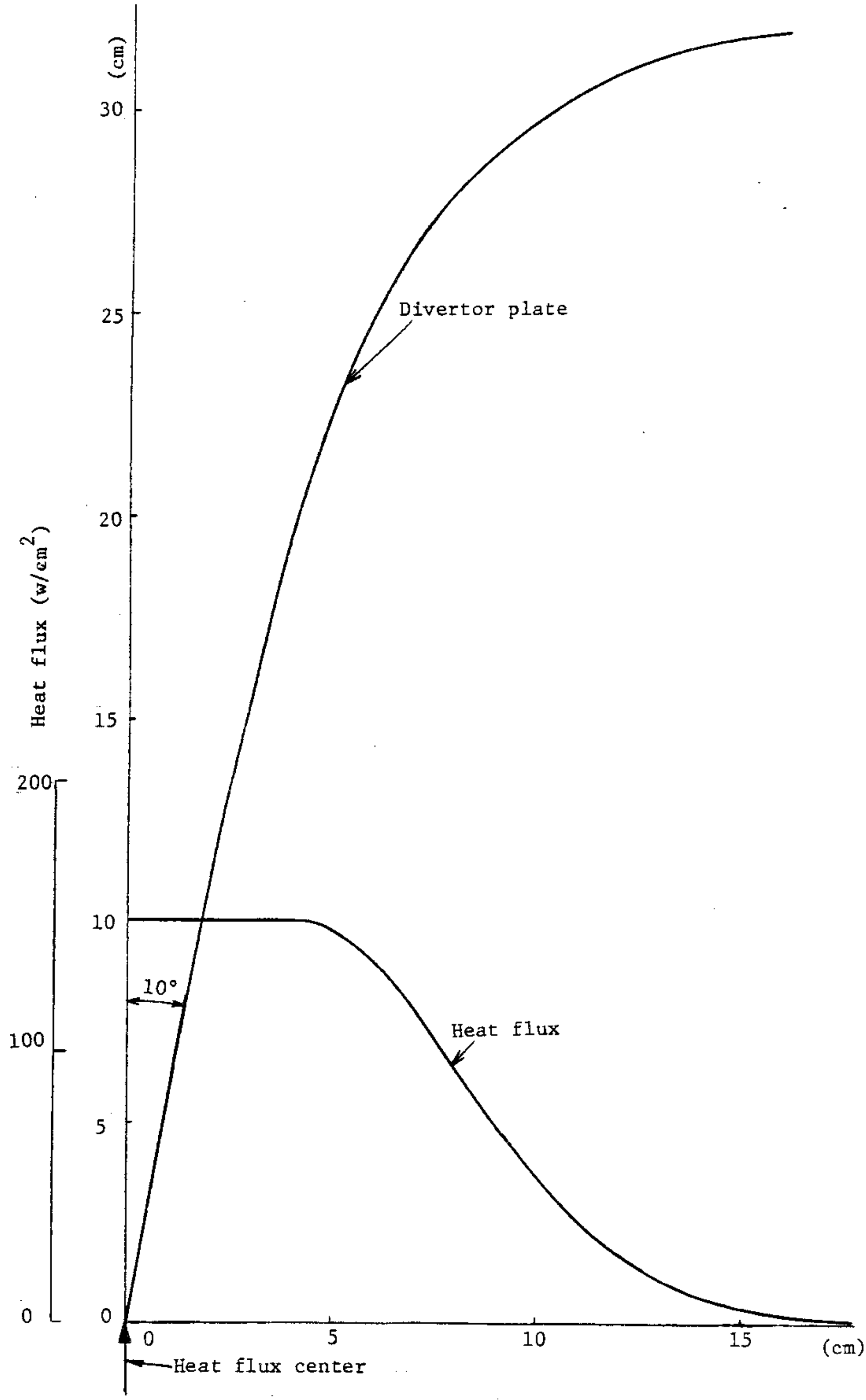

Fig. 12 Tube shape and heat flux distribution with no displacement of heat flux center

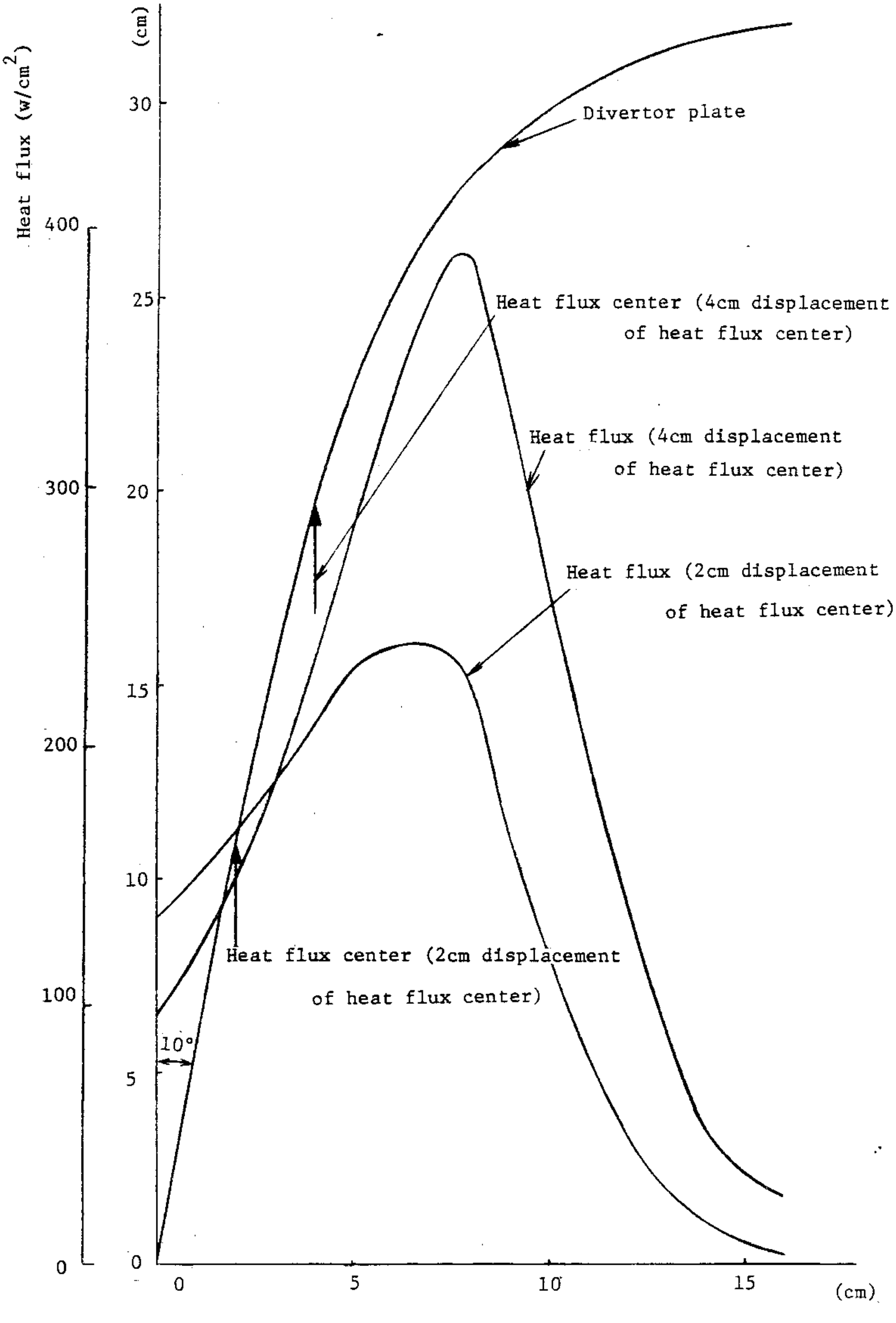

Fig. 13 Tube shape and heat flux distribution with 2cm and 4cm displacement of heat flux center

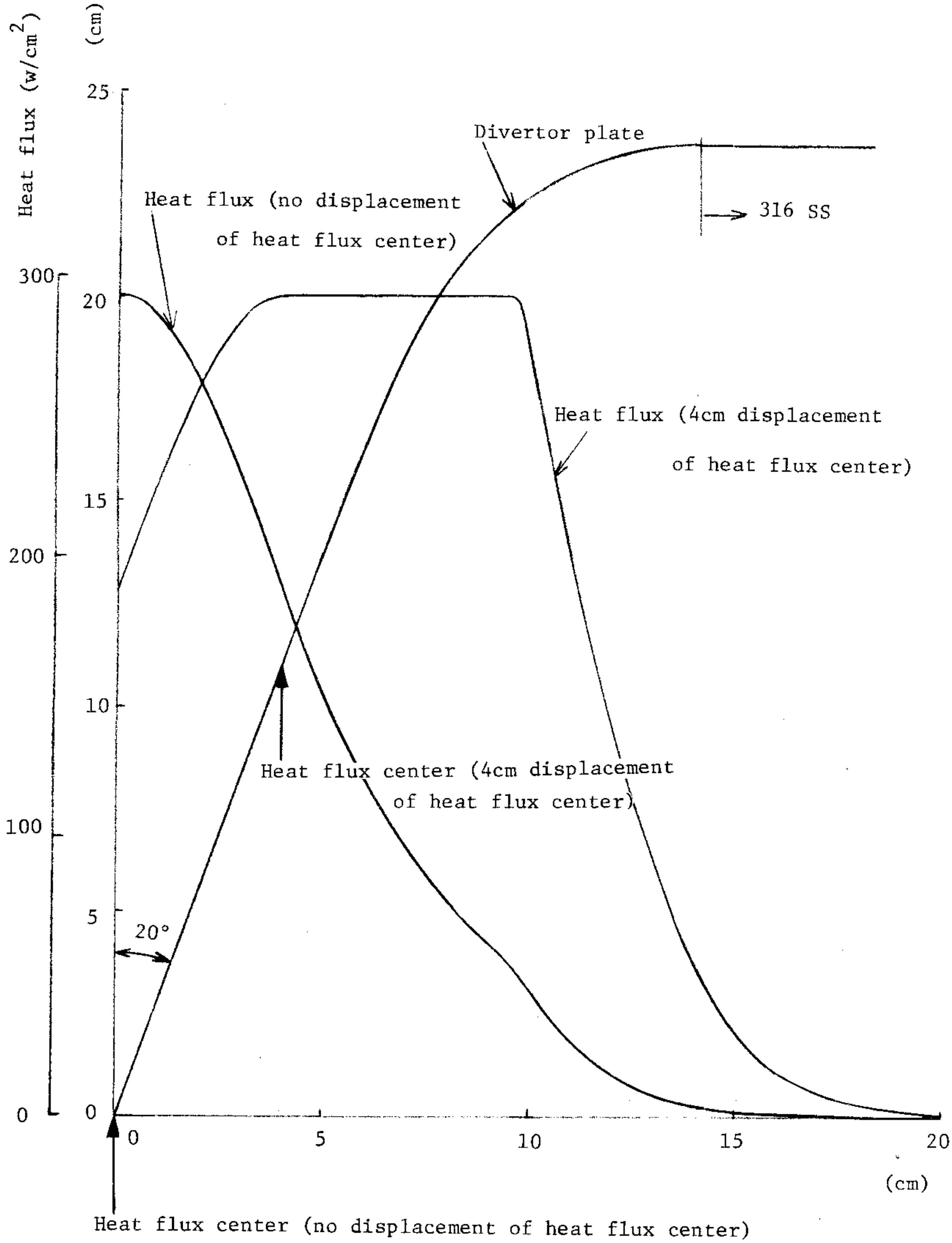

Fig. 14 Selected tube shape and heat flux distribution

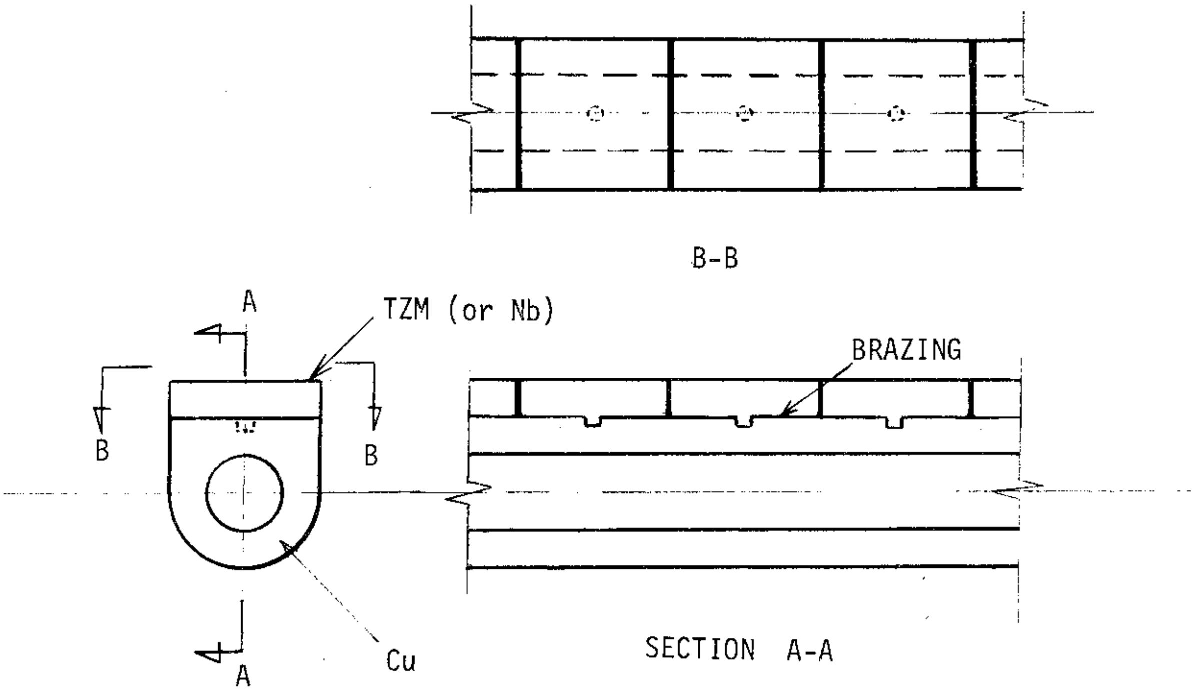

Fig. 15 An example of divertor tube

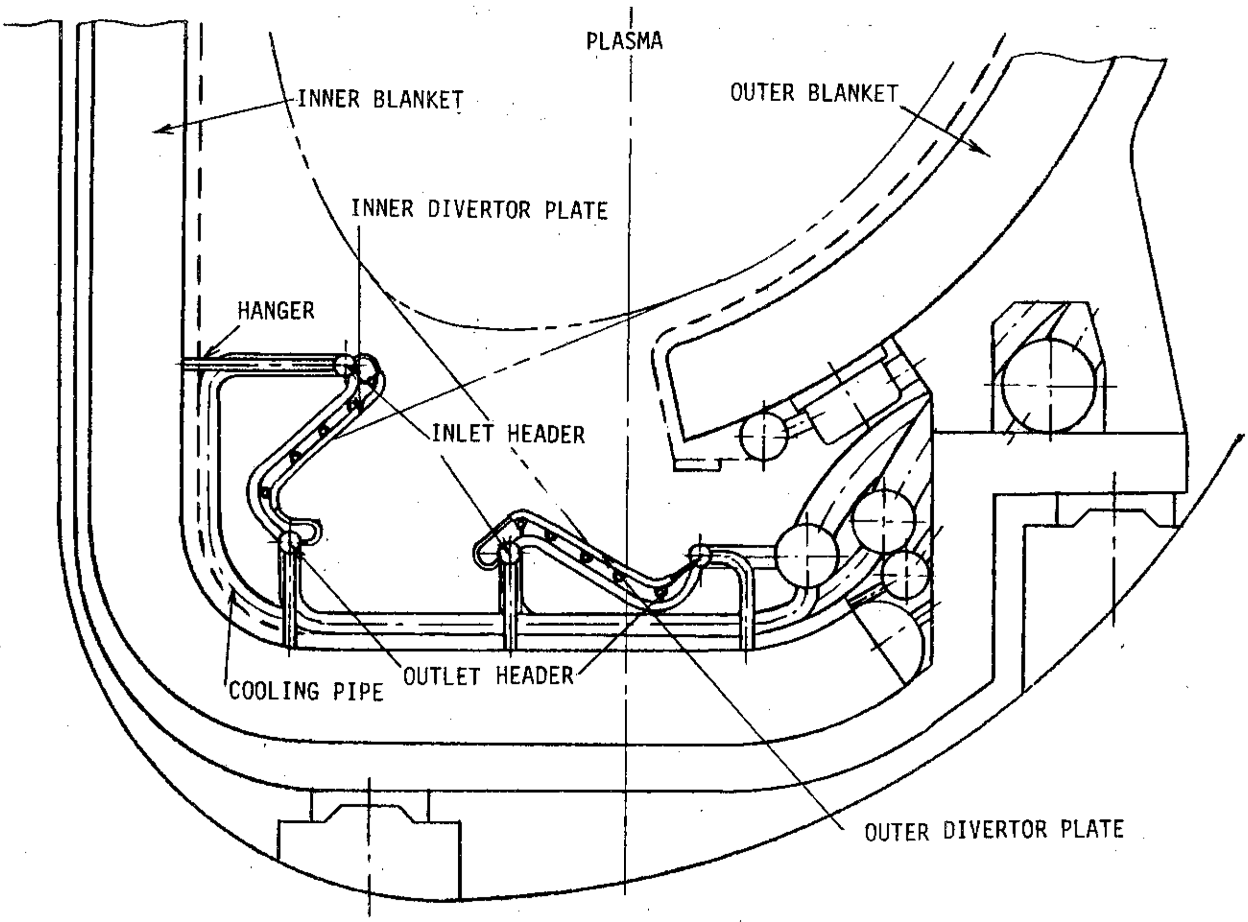

Fig. 16 Arrangement of divertor plate

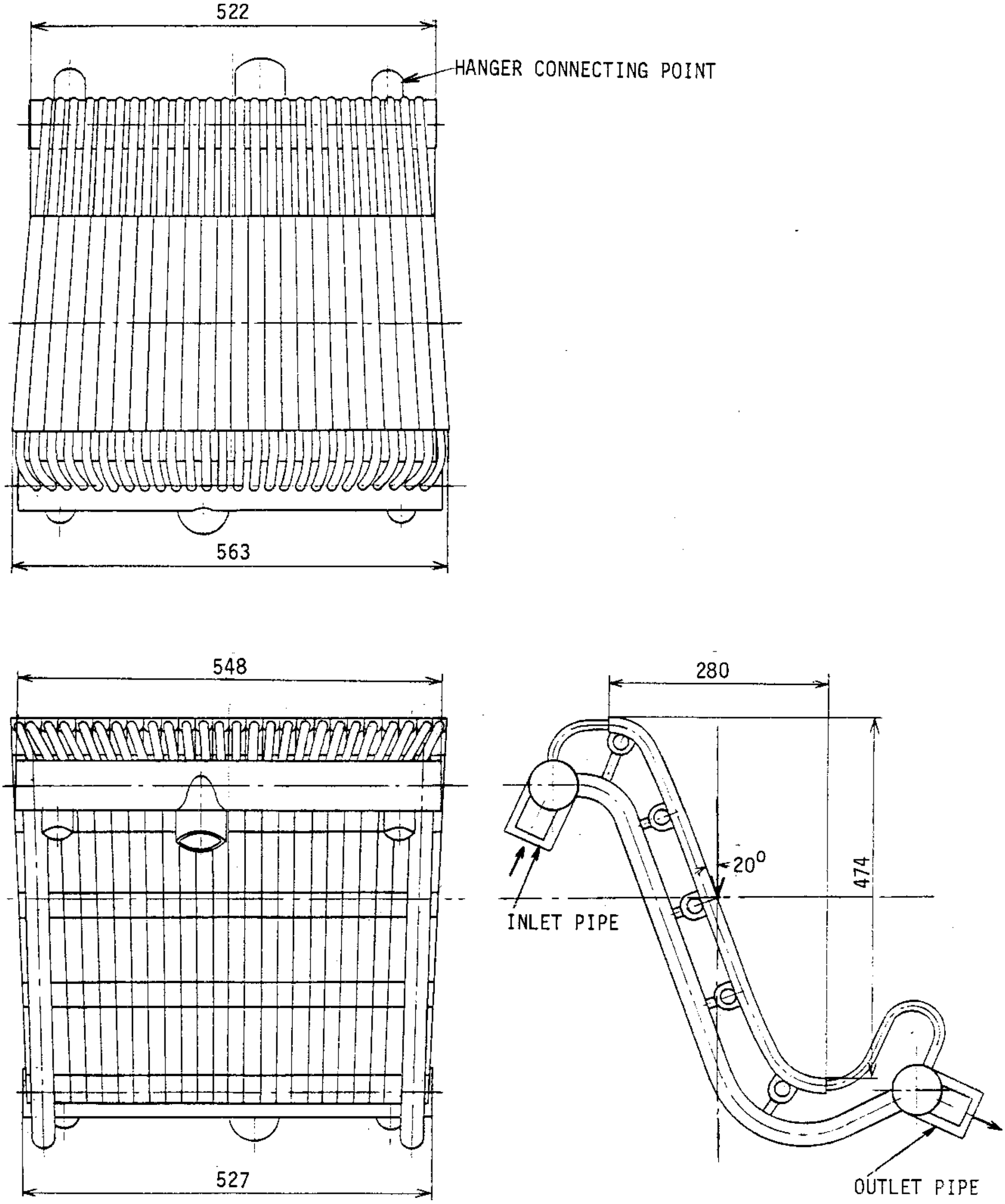

Fig. 17 Structure of inner divertor plate (tube assembly)

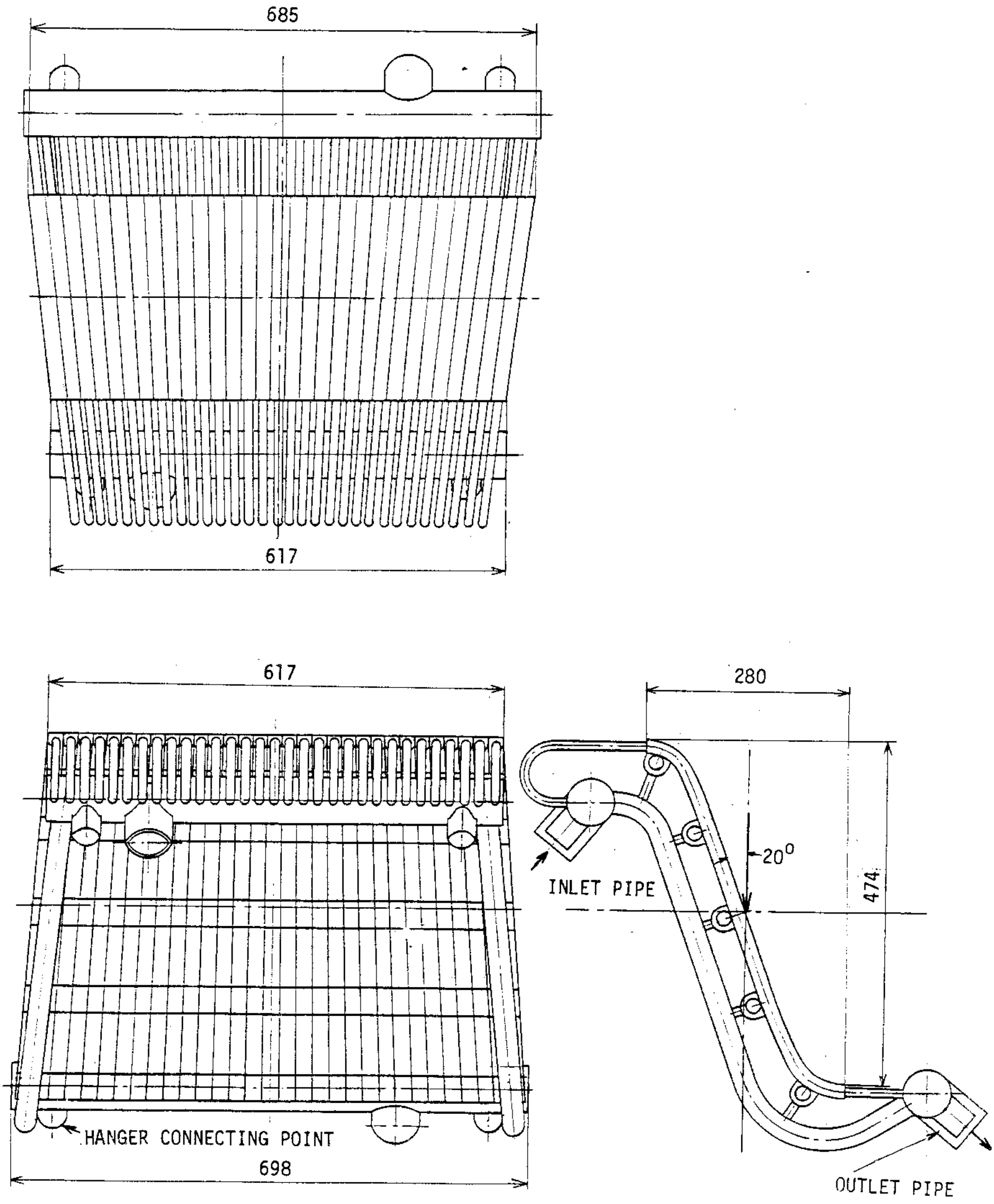

Fig. 18 Structure of outer divertor plate (tube assembly)

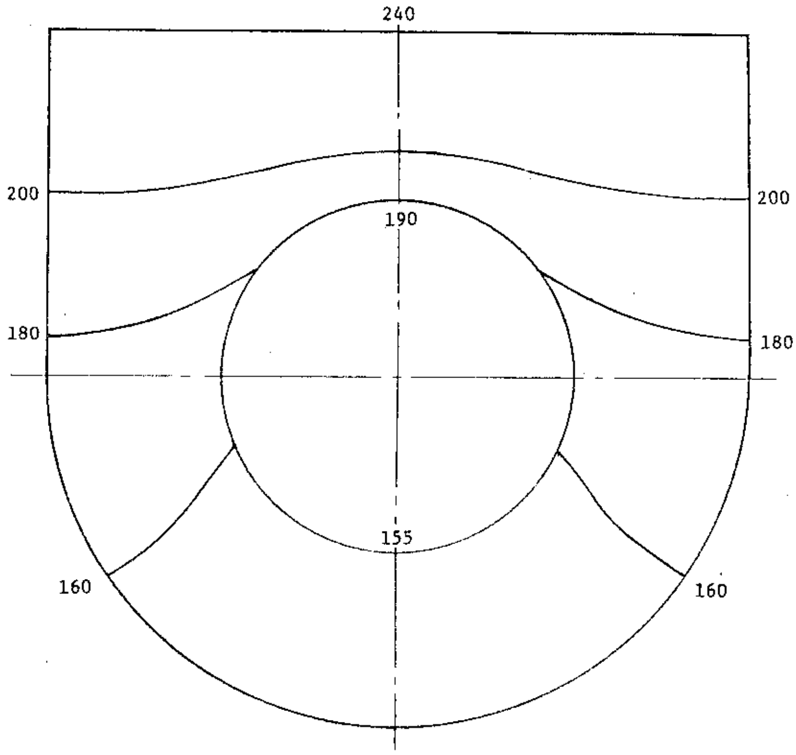

Fig. 19 Temperature distribution in the divertor tube (Rough estimation)

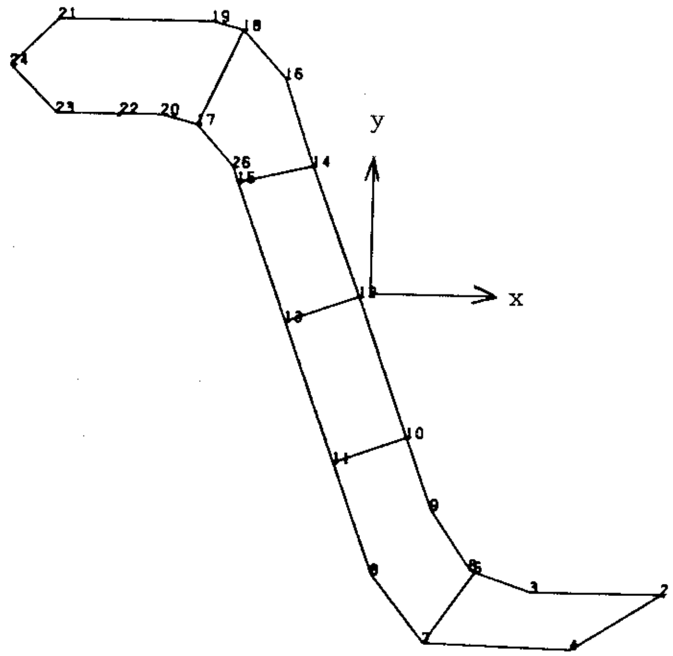

Fixed points (dx=dy=dz=0)
Node : 2,22

Fig. 20 Analytical model(2-D) of divertor structure (without support tube)

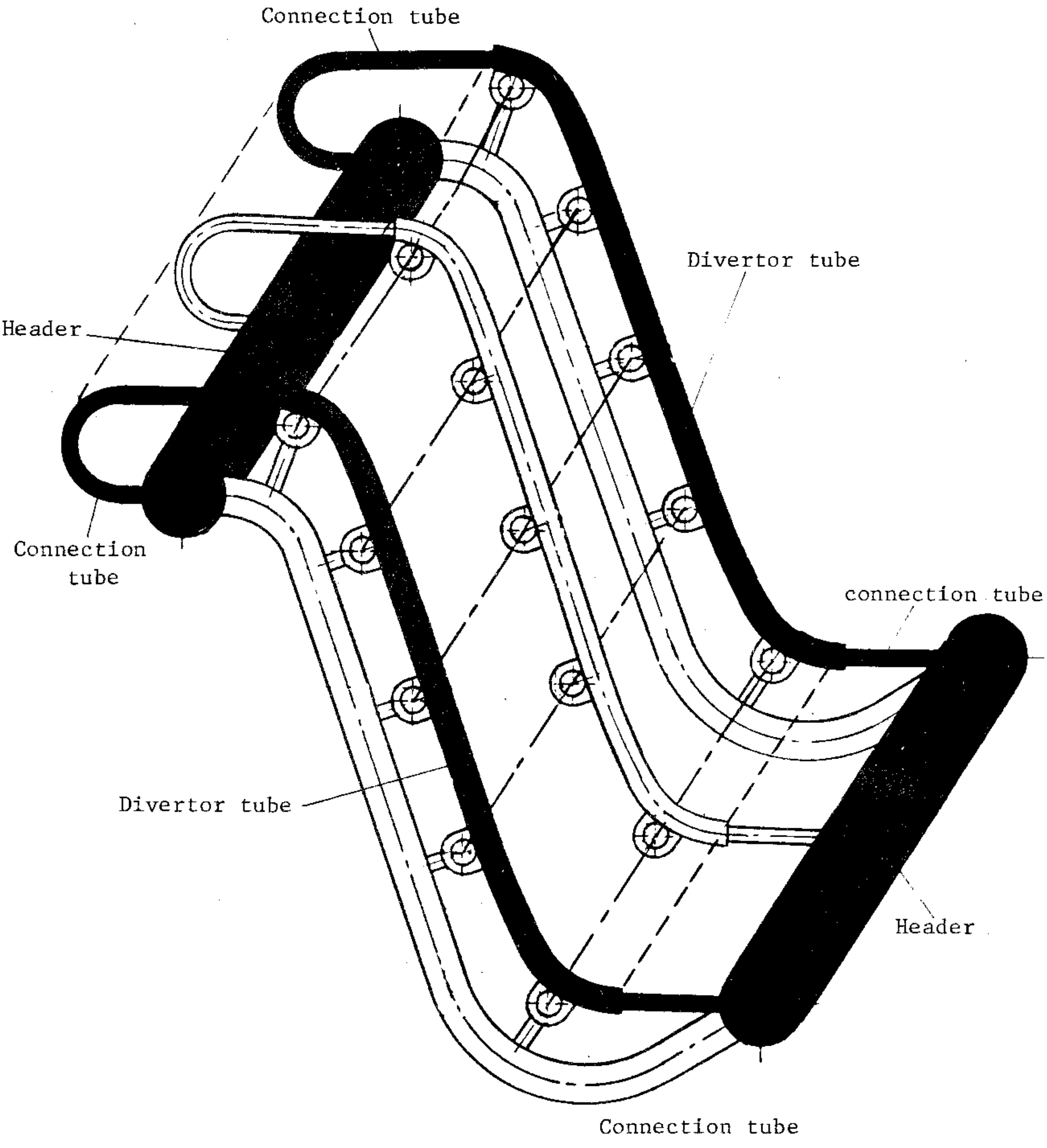

Fig. 21 Analytical model (one turn) for calculation of electro magnetic force (outer divertor plate)

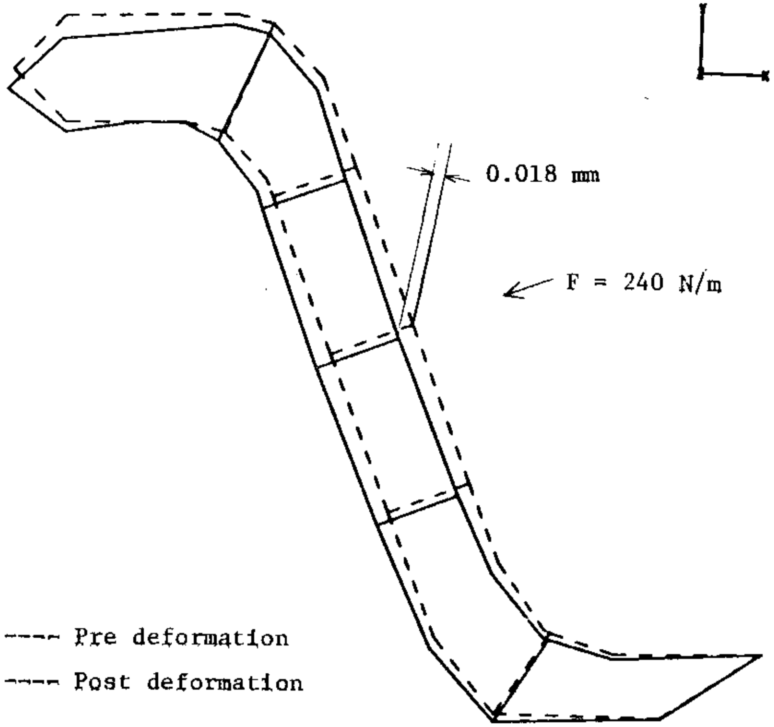

Fig. 22 Pre and post deformation shape by electro magnetic force (240 N/m)

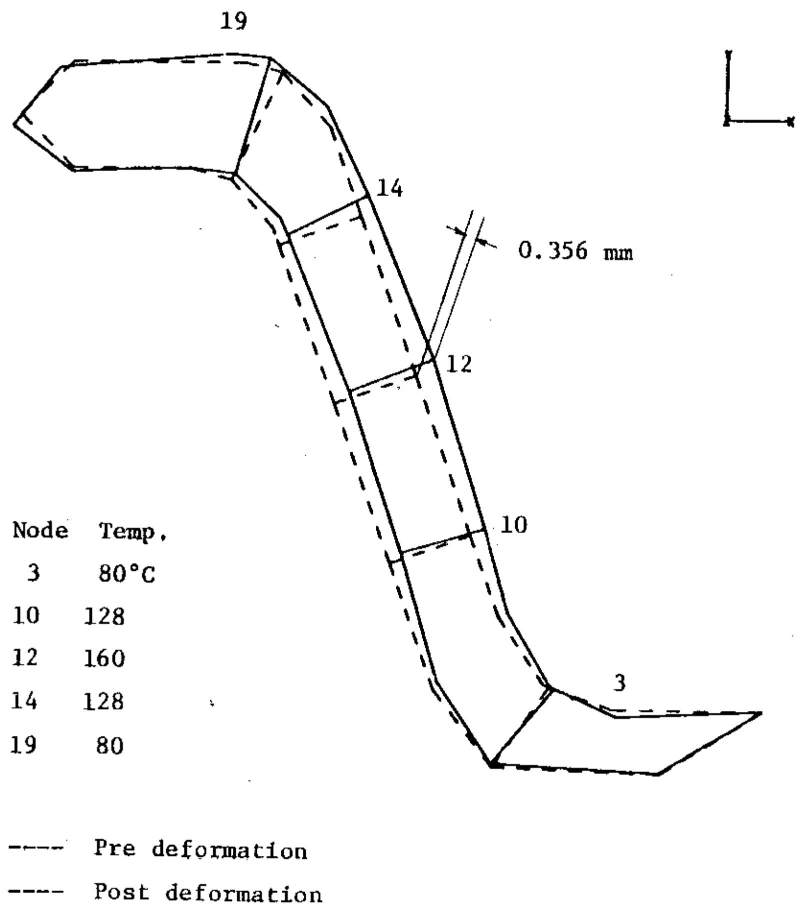

Fig. 23 Pre and post deformation shape by thermal load (max. temp. : 160°C)

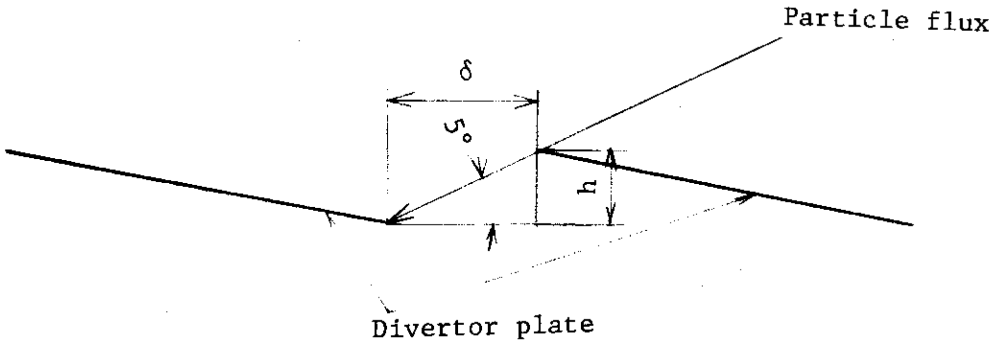

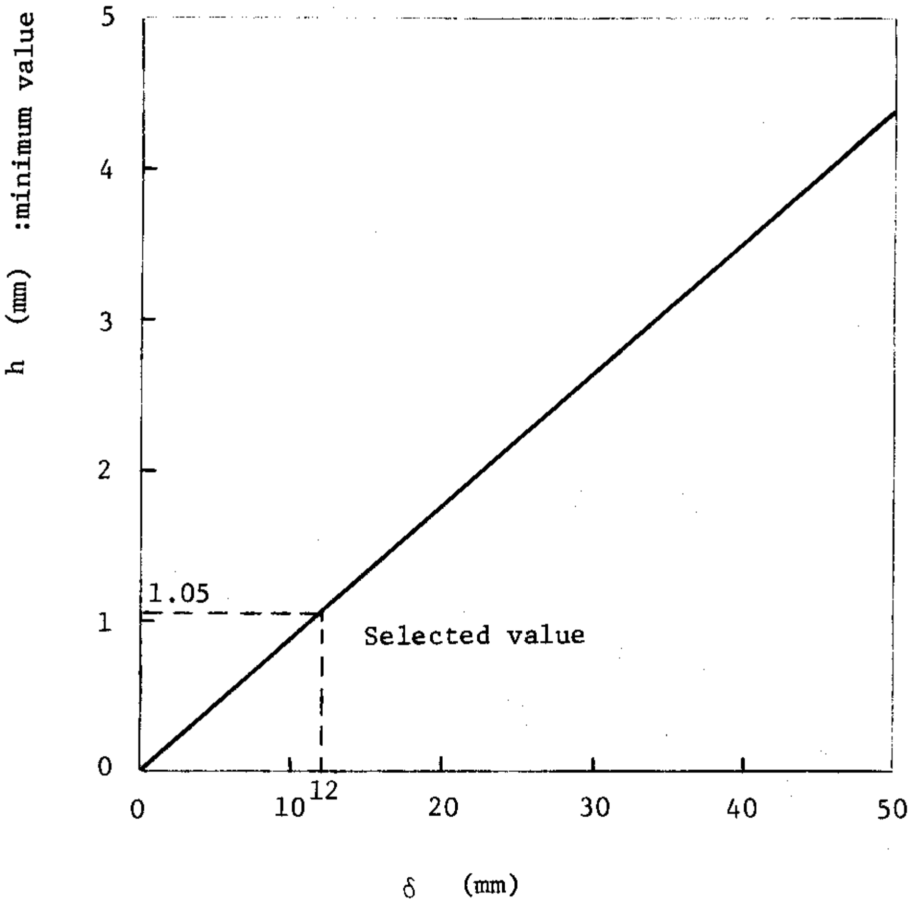

Fig.24 Gap width vs. minimum required level difference between adjacent plates

Appendix: The choice of Material for the Neutralizer Plate

Since the heat flux on the neutralizer plate is expected to be very high, strong thermal stress will be induced on the plate. Although the thermal stress also depends on the geometry and size of the plate, the thermal stress parameter , M , defined as

$$M = \frac{2\sigma_y K\ (1-\nu\ )}{\alpha\ \ E} \quad *1) \quad *2)$$

can effectively compare the thermal properties of materials.

where σ_y : yield strength

K : thermal conductivity

ν : Poissons ratio

α : coefficient of thermal expansion

E : Youngs modulus

Figure A shows the relationship of M and temperature for several materials. Large values of M are most effective in reducing thermal stress Assuming that the yield strength of copper at 200 300°C is about 7kg/mm^2 (68.6MPa), the value of M for copper will be about 200 (w/cm)

In selecting the material for the plate erosion rate radiation damage rate and fatigue of materials must be taken into account in addition of the above thermal stress parameter.

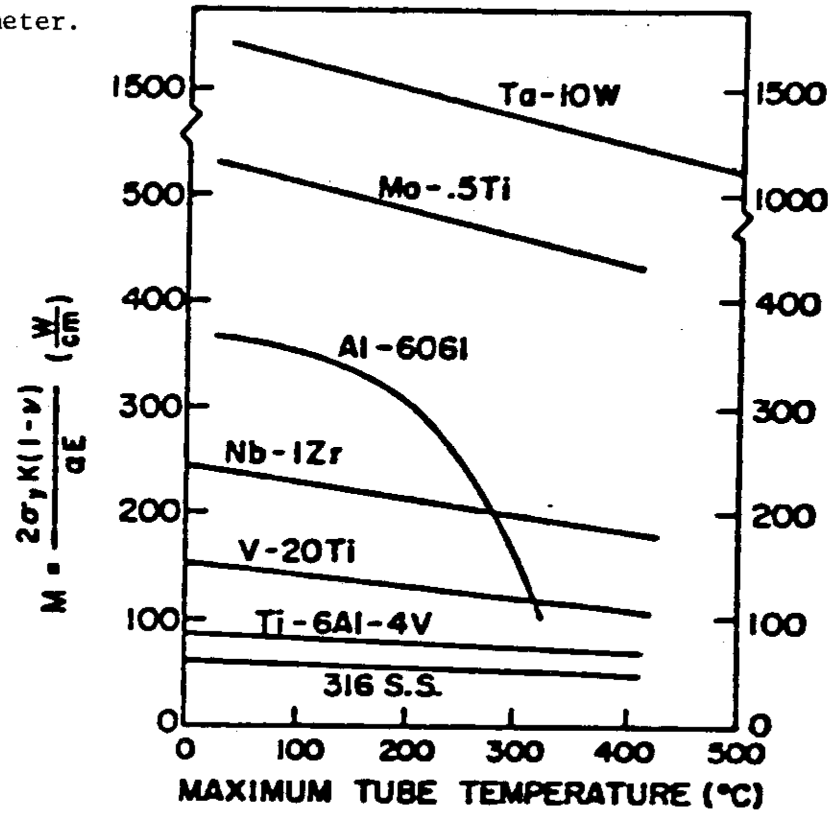

Fig.A Thermal Stress Parameter vs. Temperature *1)

*1) R.W. Conn "Tokamak Reactors and Structural Materials" UWFDM-288 (1979)

*2) A. Tobin Jour. Nucl. Mat. 85&86, (1979) pp197-201